Application of the moving epidemic method for influenza surveillance in Kunming

Yudong Gao[1], Yang Zhou[1], Siyi Luo[1], Zhengji Chen[1],
Yujue Wang[1], Zhiyan Zha[1] and Xiaoxiao Song[2]*

[1]Kunming Center for Disease Control and Prevention, Kunming, Yunnan Province, China, [2]School of
Public Health, Kunming Medical University, Kunming, Yunnan Province, China

Objective: The Moving Epidemic Method (MEM) has been widely used to assess seasonal influenza epidemics in temperate and subtropical regions. This is the first study to validate the use of MEM in a subtropical plateau environment.

Methods: This study applied the Moving Epidemic Method (MEM) to establish influenza epidemic thresholds in Kunming, China, using virological surveillance data from 2011−2012 to 2023−2024.

Results: The MEM model demonstrated high sensitivity (93%) and specificity (67%), with no detection lag for the 2023−2024 season. Epidemic thresholds (8%), which were notably lower than those in other subtropical regions, may potentially be attributed to Kunming's plateau monsoon climate.

Conclusion: This study underscored MEM's adaptability in subtropical plateau settings and provided actionable thresholds for early outbreak response.

KEYWORDS

moving epidemic method, MEM, influenza surveillance, epidemic thresholds, epidemic
intensity

1 Introduction

Influenza A and B are major causes of seasonal epidemics (1), contributing to a significant global health burden (2). Every year, influenza leads to 3–5 million cases and ~400,000 deaths globally (3) in addition to over 5 million hospitalizations. The disease burden of influenza is particularly severe during epidemic seasons, especially among vulnerable populations, such as older adults (4), young children (5), and individuals with underlying health conditions (6). In China (7), the morbidity rate of influenza in 2023 was 906.56 cases per 100,000 people, making it the most prevalent of the 41 diseases reported nationally. The estimated mortality rates due to influenza were 14.33 per 100,000 across all age groups and 122.79 per 100,000 among those aged 65 and older (8).

Four primary strains of the influenza virus—A(H1N1)pdm09, A(H3N2), B/Victoria, and B/Yamagata—have been circulating in human populations for decades (9). However, B/Yamagata has been rarely detected since March 2020 (10). Meanwhile, genetic diversity in H1N1pdm09 and B/Victoria has been increasing since April 2021, whereas H3N2 diversity has declined more gradually (10). Despite these genetic variations, the seasonal patterns of each influenza virus remain insufficiently explored (11, 12). In temperate regions, influenza typically peaks in winter, whereas subtropical and tropical regions exhibit less pronounced seasonality (13, 14). For example, northern China experiences a single seasonal influenza peak, whereas southern China often sees both a major and a minor peak (15). These regional variations are influenced by the distribution and characteristics of circulating viruses (16), making predicting epidemic timing and intensity challenging (17).

Therefore, determining the onset of an influenza epidemic is crucial for implementing effective public health interventions. Since 2004, China has implemented the China Infectious Disease Automated-Alert and Response System (CIDARS) to monitor influenza epidemics (18). Although climate change and mutations introduce uncertainties, seasonal influenza still exhibits repeatability and structural characteristics, and key patterns can be identified based on historical data. Various approaches (18, 19) have been proposed to detect influenza epidemics, including the cumulative sum (CUSUM), serial regression, and Moving Epidemic Method (MEM), among others. The MEM initially proposed by Vega et al. (20) has been widely recognized as an effective tool for defining epidemic and non-epidemic periods based on routine surveillance data. MEM has been well-documented in temperate (21–23) and subtropical regions (24, 25). Similarly, the results showed that the prediction error from the actual epidemic week was only ±1 week in Respiratory Syncytial Virus (RSV) (26) verifying the robustness of MEM in different diseases and data sources.

To date, the potential application of MEM in detecting influenza epidemics in subtropical plateau regions remains underexplored. This study is the first to validate MEM in a subtropical plateau city.

2 Materials and methods

2.1 Study area and data sources

Kunming, located in Southwestern China, is the capital city of Yunnan Province with a resident population of 8.69 million as of the end of 2024. Administratively, Kunming consists of 14 county-level divisions, including 7 districts, 6 counties, and 1 county-level city. The four sentinel surveillance sites were established in response to the 2003 following Severe Acute Respiratory Syndrome (SARS) outbreak, based on two considerations: (1) multiple administrative levels of hospitals, including provincial, municipal, and county-level facilities, and (2) key hospital types: general hospitals, children's hospitals, and infectious disease specialty hospitals. By the end of 2024, four national sentinel hospitals remained unchanged from their establishment. They were actively conducting influenza surveillance: the First Affiliated Hospital of Kunming Medical University (102key ho 25 county the Third People's Hospital of Kunming(102he Thi 25nming(1 the Children's Hospital of Kunming(102en's H 24nming(1 and the First People's Hospital of Anning (102 the F 2402 the (Figure 1). Each sentinel hospital collected a minimum of 20 respiratory specimens per week from individuals presenting with influenza-like illness (ILI). An influenza-like illness (ILI) case was defined as a fever (body temperature ≥ 38°C) accompanied by either a cough or a sore throat. The collected specimens were sent to reference laboratories for influenza virus analysis, where reverse transcription polymerase chain reaction (RT-PCR) was conducted to determine influenza virus subtypes within the same week of sample collection. The laboratory results were electronically submitted to the web-based National Influenza Surveillance Information System (NISIS). The confirmed influenza case data, sourced from China's infectious disease surveillance system (CIDS), and demographic data come from the official website of the National Bureau of Statistics.

Based on historical seasonal epidemic patterns in Kunming, influenza is most prevalent during the winter and spring months. To optimize the MEM analysis by focusing on epidemiologically meaningful data, we defined the monitoring period from the 40th week of the current year to the 30th week of the following year, covering a total of 43 weeks per influenza season. This period encompasses the entire phase of substantial influenza transmission in Kunming, excluding weeks 31–39, during which there was minimal activity. In addition to the overall influenza positivity proportion (PR), the weekly PRs of A(H1N1)pdm09, A(H3N2), B/Victoria lineage, and B/Yamagata lineage were also calculated separately. This study included 10 influenza seasons from 2011–2012 to 2019–2020, as well as the 2023–2024 season, for analysis using the MEM.

2.2 Cross-correlation analysis

A spatiotemporal analysis was conducted to examine the geographic and temporal distribution of influenza incidence in Kunming from 2010 to 2020. To assess the temporal relationship between PR and incidence rate, a cross-correlation function (CCF) analysis was conducted using weekly data from 2010 to 2024. Pearson correlation coefficients were calculated at lags from −5 to +5 weeks to determine whether PR could serve as a leading indicator of incidence rate. The analysis was performed across four periods: the full dataset (2010–2024), the pre-pandemic years (2010–2019), the post-pandemic years (2023–2024), and a filtered set excluding 2020–2022.

2.3 Moving epidemic method

The Moving Epidemic Method (MEM) is a three-step process used to define the start, length, and end of each influenza epidemic season.

Step 1: Determining the Epidemic Period.

The epidemic period is defined as the time when the cumulative monitoring index first drops below a predefined threshold δ, expressed as a percentage of the total cumulative monitoring index for the season. The length of the epidemic period is determined using the Maximum Accumulated Percentage (MAP), which identifies the minimum number of consecutive weeks that account for the highest cumulative percentage of influenza cases, as described by Vega et al. (20), each influenza season is divided into three distinct periods: the pre-epidemic period, the epidemic period, and the post-epidemic period. In this study, MAP represents the maximum value of the cumulative percentage of PR over a specific period within a flu season, relative to the total cumulative positivity rate for the entire season. The particular calculation formulas are as follows:

$$t_j^r = \max_{k=1,\ldots,S-r+1}\left\{\sum_{i=k}^{k+r-1} t_{i,j}\right\}, \forall r = 1,\ldots,S \quad (1)$$

$$t_j^s = \sum_{i=k}^{S} t_{i,j} \quad (2)$$

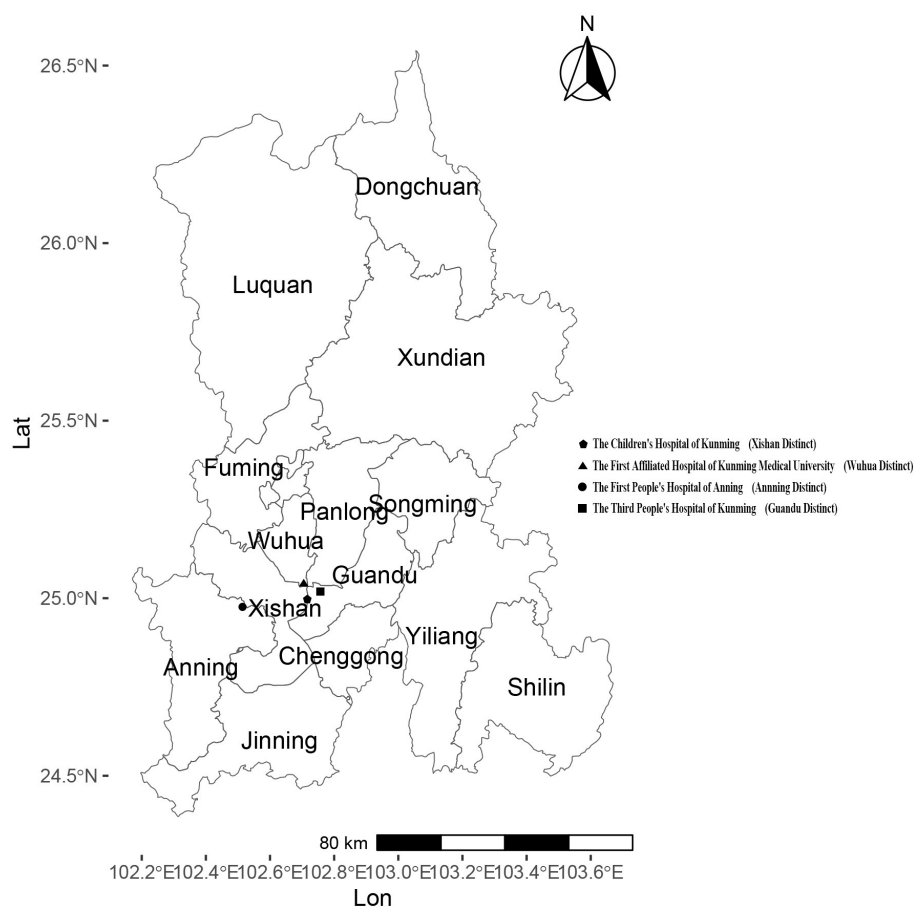$$P_j^r = \frac{t_j^r}{t_j^s} \quad (3)$$

FIGURE 1
Distribution of 14 counties/districts and 4 sentinel hospitals in Kunming.

The MAP curve draws the maximum cumulative rate for a period of a given length r, expressed as a percentage of the total rate of P_j^r of the total rate of the j season. The t_j^r is the highest accumulated rate among j epidemic in r period. The t_j^s is the accumulate rate in the j season. The $t_{i,j}$ is the i rate of the j season, and S is the monitoring weeks in each season. The k is the number of start weeks of consecutive r weeks.

Step 2: Calculation of Epidemic Thresholds

The epidemic thresholds are calculated based on PR from both the pre-epidemic and post-epidemic periods. The top n-values (where n = 30/N) with the highest PR in both the pre-epidemic and post-epidemic periods are selected for analysis. The 95% one-sided confidence interval (CI) upper limit of the arithmetic mean of these 30 values is used to define the Pre-epidemic and post-epidemic thresholds.

Step 3: Classification of Epidemic Intensity

The epidemic intensity is categorized based on PR values observed during the epidemic period. The top n-values (where n = 30/N) with the highest positivity rates in each epidemic period are selected for analysis. The 40, 90, and 95% one-sided confidence intervals (CIs) upper limits for the geometric mean of these 30 values are used to define the thresholds for: moderate intensity, high intensity, and very high intensity.

2.4 Model evaluation

The MEM model can be used to classify each season into three periods, namely, pre-epidemic, epidemic, and post-epidemic periods. The rates in the pre-epidemic period were expected to be lower than the pre-epidemic threshold rate, whereas rates during the epidemic period were expected to be higher. Rates in the post-epidemic period were expected to be lower than the post-epidemic threshold rate. For the 2023–2024 season, the epidemic threshold and intensity levels (moderate, high, and very high) were determined based on historical pre-epidemic, post-epidemic, and epidemic values from the 2011–2012 to 2019–2020 seasons.

The MEM model was implemented using RStudio 4.2.1, and its performance was assessed through calculations of sensitivity, specificity, and timeliness. A true positive week is defined as a week within the epidemic period when the PR exceeds both the start- and post-threshold. A true negative week is a week within the pre- or post-epidemic period where the PR is below the threshold. Sensitivity is calculated as the number of true positive weeks divided by the total number of weeks in the epidemic period. Specificity is the number of true negative weeks divided by the total number of weeks in the non-epidemic period. Youden's index is the

FIGURE 2
Time series of influenza incidence rate in Kunming, 2010–2024.
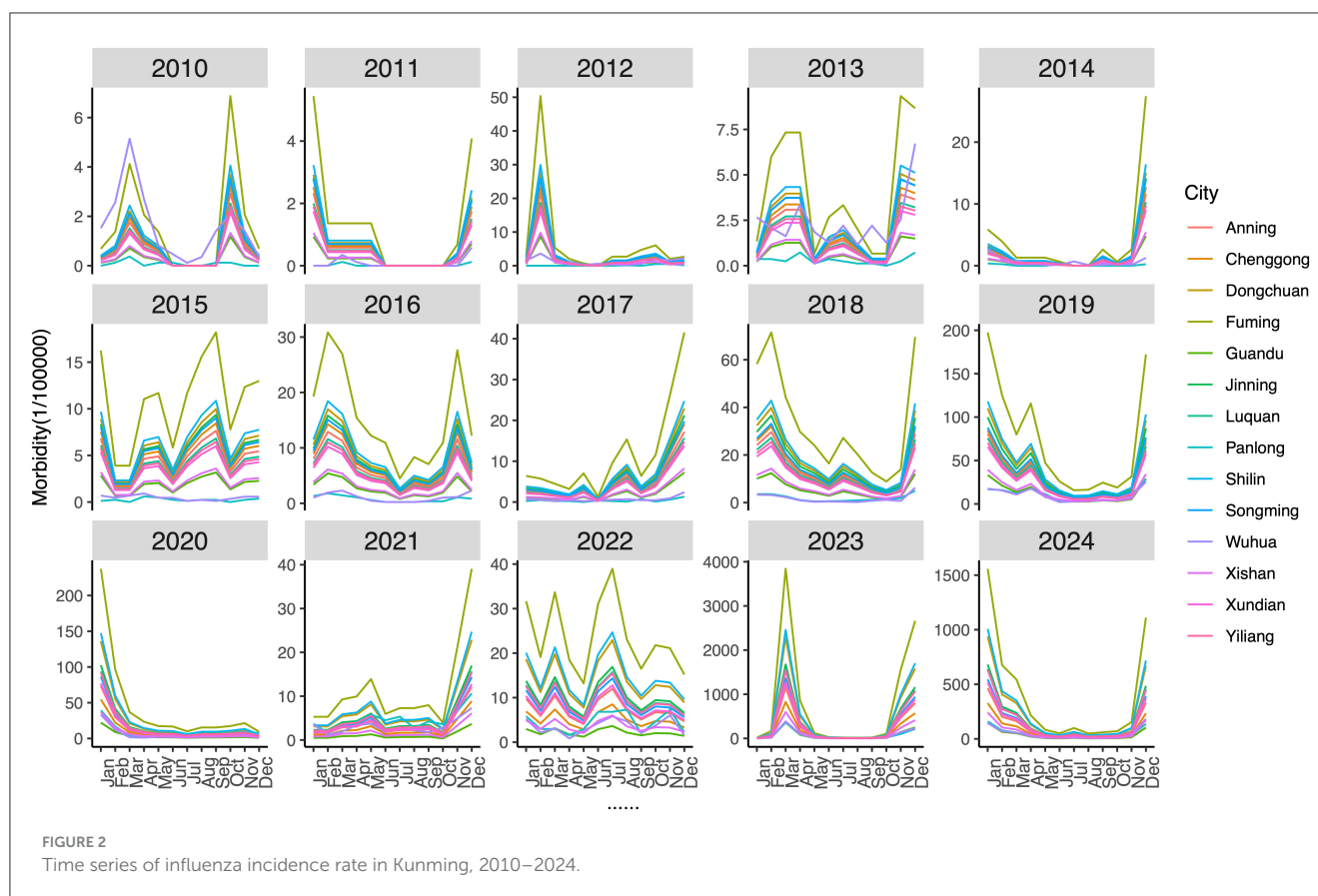
sum of sensitivity and specificity minus one. Timeliness was defined as the number of weeks between the first occurrence of a positive proportion exceeding the established epidemic threshold and the first week of the MEM-defined epidemic period. The threshold parameter δ was iteratively adjusted, with an initial value of 1.0, a final value of 3.0, and a step size of 0.1. The optimal value of δ was selected based on its performance in terms of sensitivity, specificity, and Youden's Index.

The optimized MEM model was subsequently employed to determine the epidemic threshold and intensity thresholds, which were then applied to assess the epidemic intensity of the 2023–2024 winter-spring influenza season in Kunming. For a target type of influenza virus, an epidemic threshold was calculated using the seasons when the proportion of the target strain exceeded 25%.

2.5 Cross-validation analysis

The cross-validation procedure was employed to evaluate the performance of MEM. Each influenza season is treated individually as the target season, while other seasons serve as a historical baseline for comparison. The MEM model's first and second steps are applied to calculate the epidemic start- and post-thresholds for the target season. The actual weekly PR during the season was compared with the pre-epidemic, epidemic, and post-epidemic

periods, as well as the start and post-thresholds determined by the MEM model. Sensitivity, specificity, and Youden's index are then calculated.

3 Results

3.1 Seasonal influenza activity in Kunming

The annual and seasonal analysis of influenza incidence rate across 14 districts and counties of Kunming from 2010 to 2024 revealed substantial heterogeneity in both intensity and distribution over time. Time–series plot (Figure 2) shows a clear seasonal pattern, with influenza incidence typically peaking during the winter and early spring months (January to March). From 2010 to 2018, morbidity levels in most regions remained relatively low and stable, with peak values generally below 500 cases per 100,000 population. However, a sharp increase in incidence was observed after 2018, particularly in peripheral districts–countries, Fuming, Shilin, Dongchuan, and Jingning. The decline in morbidity between 2020 and 2022 is notable across all districts, aligning with the period of coronavirus disease 2019 (COVID-19) control measures, which likely reduced the spread of influenza. However, this was followed by an unprecedented resurgence in 2023–2024, with many peripheral districts reporting incidence levels exceeding 3,000–9,000 per 100,000, far above pre-pandemic norms. Spatial distribution maps (Figure 3) further

FIGURE 3
Spatial distribution of influenza incidence rate in Kunming, 2010–2024.
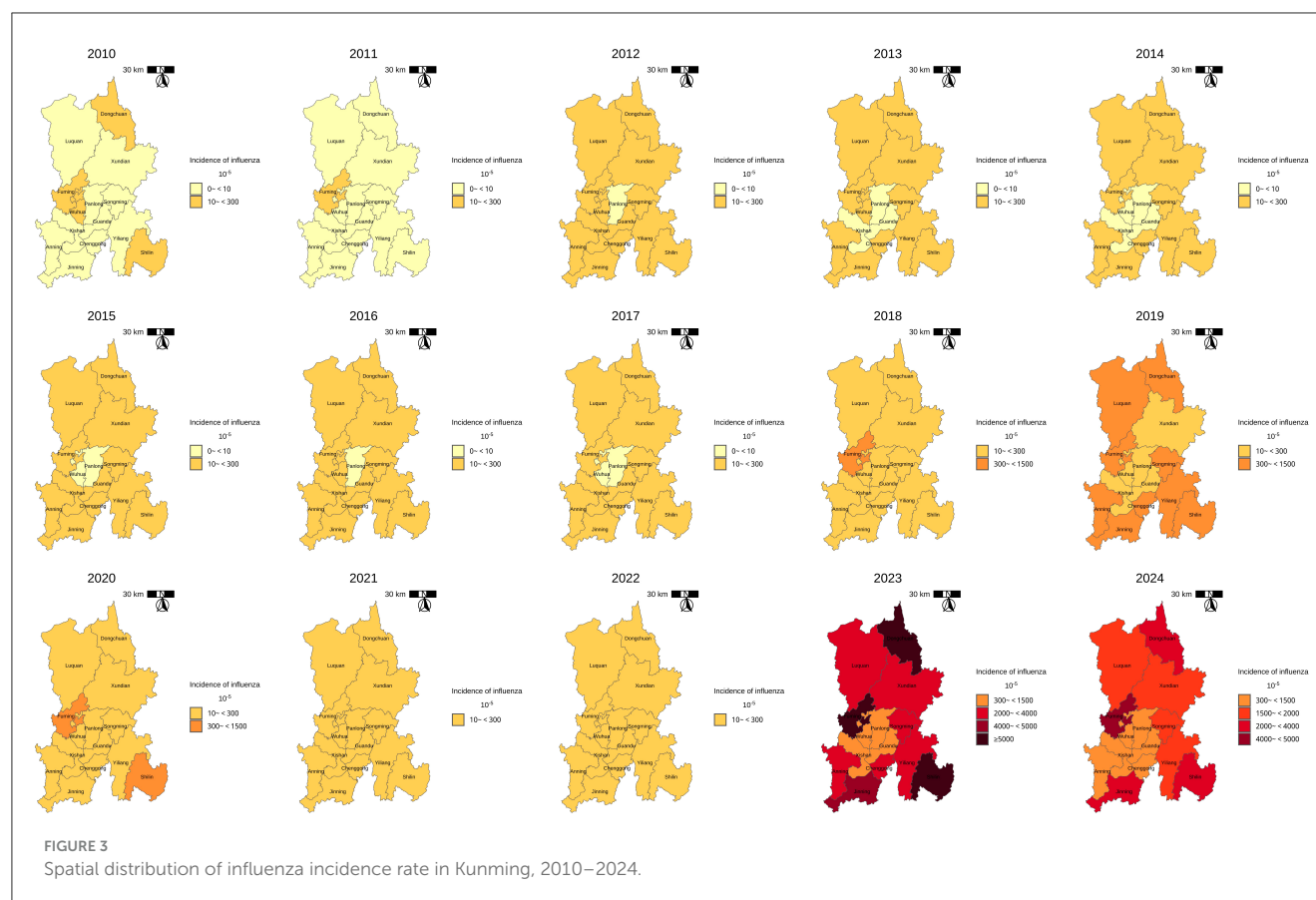
highlight this post-pandemic intensification and concentration. Prior to 2018, the majority of the regions exhibited modest rates (<300/100,000), with minimal spatial disparity. In contrast, by 2023, regions such as Dongchuan, Fuming, Luquan, Shilin, and Yiliang formed a clear belt of high-morbidity clusters, particularly in the northeast and southeast of Kunming. Central urban districts, such as Wuhua, Panlong, and Guandu, maintained relatively lower incidence levels throughout the study period (Table 1).

Regarding the virological data, the peak PR ranged from 24.63 to 71.62%. The weekly PR exhibited seasonal trends, typically peaking either at the beginning or the end of the year. The peak timing varied between seasons (Figure 4) and predominantly followed a unimodal distribution, except for the 2017–2018 and 2018–2019 seasons, which showed a clear bimodal pattern. The dominant influenza strains also varied from one season to another. A(H1N1)pdm09 was the predominant strain in the majority of the seasons, particularly in 2012–2013, 2013–2014, 2017–2018, 2018–2019, and 2019–2020, with positivity rates exceeding 45%. A(H3N2) was prevalent in the seasons 2014–2015, 2016–2017, 2019–2020, and 2023–2024, with a positivity rate exceeding 45% in each of these seasons. B/Victoria was the dominant strain in the 2011–2012 season, accounting for 72.6% of positive cases. B/Yamagata was most prevalent in the 2023–2024 season, making up 45.58% of positive cases (Table 2).

3.2 Cross-correlation analysis

The cross-correlation analysis demonstrated that PR consistently showed a statistically significant positive correlation with incidence rate, often with a one-week lead. During the whole study period from 2010 to 2024, the strongest correlation ($r = 0.54$) was observed at a lag of -1 week. When the COVID-19 pandemic years (2020–2022) were excluded, the correlation increased slightly ($r = 0.57$), still at a lag of -1 week. In the pre-COVID-19 pandemic period (2010–2019), the peak correlation ($r = 0.59$) occurred at a zero lag, indicating a contemporaneous relationship. In contrast, the post-COVID-19 pandemic period (2023–2024) showed a robust correlation ($r = 0.90$) at a lag of -1 week, suggesting that PR became a highly reliable early indicator of morbidity trends in the aftermath of the COVID-19 pandemic (Figure 5).

3.3 Parameter selection

Under different δ values, the sensitivity ranges from 0.29 to 0.74, the specificity ranges from 0.87 to 0.98, the Positive Predictive Value (PPV) ranges from 0.75 to 0.89, the Negative Predictive Value (NPV) ranges from 0.71 to 0.86, and the Youden index (YI) ranges from 0.26 to 0.61. The parameter $\delta = 1.1$ yields the best performance with the highest sensitivity, NPV, and

TABLE 1 Annual influenza incidence rate per 100,000 population in 14 districts of Kunming, 2010−2025.

City	2010	2011	2012	2013	2014	2015	2016	2017	2018	2019	2020	2021	2022	2023	2024
Fuming	19.24	15.65	81.88	50.00	47.71	136.36	186.26	138.66	396.58	870.44	518.37	136.42	283.83	9,405.64	4,672.57
Shilin	11.37	9.27	48.61	29.53	28.52	81.40	111.37	82.60	237.59	520.30	321.81	86.26	179.84	6,018.03	3,018.65
Dongchuan	10.30	8.39	44.36	27.08	26.16	74.73	102.55	76.68	220.77	485.61	297.23	79.81	166.86	5,595.71	2,813.51
Jinning	9.87	8.07	41.92	25.51	24.58	70.00	95.61	70.82	202.78	439.78	223.82	59.33	123.28	4,100.86	2,043.33
Luquan	7.06	5.76	30.35	18.52	17.89	51.09	70.07	52.39	151.27	333.74	204.55	54.76	114.54	3,834.62	1,925.11
Yiliang	6.68	5.44	28.64	17.48	16.90	48.39	66.38	49.34	141.57	309.76	201.36	53.81	112.57	3,765.22	1,888.86
Songming	9.75	7.96	41.92	25.42	24.25	67.52	91.11	65.98	183.82	387.68	188.60	50.12	104.47	3,328.62	1,638.14
Xundian	6.13	5.00	26.35	16.13	15.63	44.87	61.69	45.96	131.89	289.78	168.21	44.59	92.91	3,095.99	1,545.02
Anning	8.20	6.69	34.76	21.01	20.17	57.22	77.89	57.47	164.57	355.78	160.21	42.39	87.51	2,829.29	1,392.45
Chenggong	9.01	7.26	37.89	23.01	22.12	63.25	86.23	63.69	177.57	372.95	119.32	30.97	61.90	2,022.40	982.07
Xishan	3.71	3.02	15.86	9.72	9.42	26.96	36.99	27.50	79.10	173.54	80.67	21.33	43.94	1,459.97	724.49
Wuhua	18.94	1.04	15.02	28.97	7.74	5.75	12.60	8.00	19.93	120.45	77.51	37.55	42.20	926.38	582.37
Kunming	2.52	1.06	7.15	8.28	3.67	7.65	12.69	7.99	25.43	82.19	55.11	24.06	37.45	804.86	567.40
Panlong	0.99	0.25	1.22	3.65	1.09	3.01	9.59	4.66	22.92	137.00	104.86	56.21	53.42	895.95	563.89
Guandu	3.28	2.67	14.09	8.62	8.35	23.81	32.67	24.15	68.61	146.63	48.37	12.79	26.49	880.82	438.00

FIGURE 4
Weekly influenza positivity rates (PR) and MEM-defined epidemic periods in Kunming, from 2011–2012 to 2023–2024. Curves from bottom to top: All types, A(H3N2), A(H1N1)pdm09, B/Yamagata, and B/Victoria.
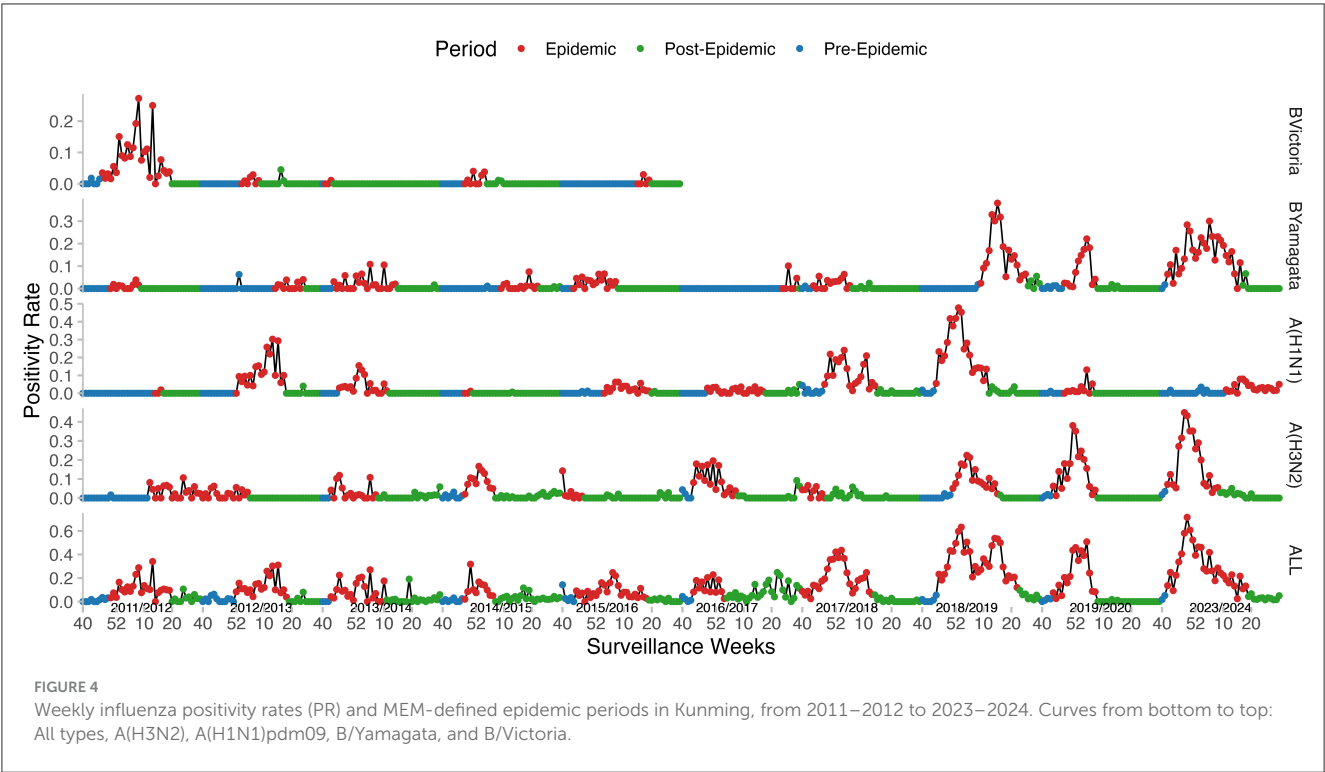
TABLE 2 Virological characteristics of influenza in Kunming from 2011–2012 to 2023–2024 seasons.

Seasons	PR peak		Percentage of Positive specimens (%)			
	Week	Value (%)	A(H1N1)pdm09	A(H3N2)	B/Yamagata-lineage	B/Victoria-lineage
2011–2012	13	34.09	0.63	20.89	4.43	74.05
2012–2013	15	31.03	81.60	12.80	5.60	0.00
2013–2014	5	27.23	45.26	29.93	24.82	0.00
2014–2015	50	31.76	1.39	86.11	12.50	0.00
2015–2016	6	24.63	35.96	20.18	34.21	9.65
2016–2017	22	24.74	16.96	75.45	7.14	0.45
2017–2018	2	43.64	69.15	14.54	11.70	4.61
2018–2019	2	63.28	54.45	19.28	25.82	0.45
2019–2020	4	50.82	8.43	66.01	25.56	0.00
2023–2024	49	71.62	9.34	45.08	45.58	0.00

YI (Table 3). The sensitivity, specificity, PPV, NPV, and Youden index are 0.74, 0.87, 0.76, 0.86, and 0.61, respectively. Therefore, $\delta = 1.1$ was selected as the optimal parameter and applied in subsequent analyses.

3.4 Cross-validation of MEM

For the 2023–2024 season, the sensitivity, specificity, and YI were 0.93, 0.67, and 0.6, respectively. By the cross-validation process, the 2014–2015 season has the lowest sensitivity and YI. After excluding the data from the 2014–2015 epidemic season, the MEM models of each epidemic season performed well (Table 4).

The data from 9 epidemic seasons (except 2014–2015) were finally included.

3.5 MEM for influenza seasons in Kunming

The onset of the epidemic varied across seasons, ranging from week 40 to week 52, while the epidemic duration ranged from 11 to 29 weeks. The pre-epidemic threshold values were relatively stable, fluctuating between 5.49 and 8.10%. However, the thresholds for medium, high, and very high intensity exhibited noticeable variation across seasons. The majority of the seasons recorded medium or low intensity levels, except for 2018–2019, which was

FIGURE 5
Temporal trends of influenza incidence rate and PR in Kunming, 2010–2025.
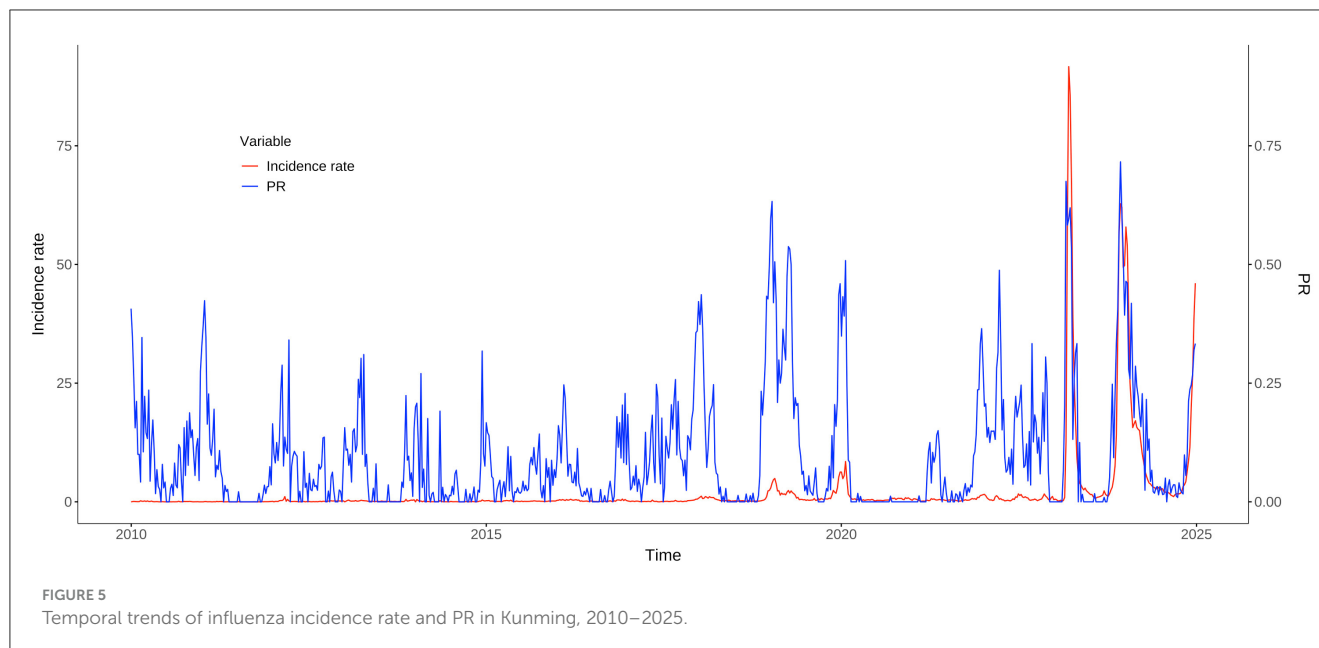
classified as high intensity, and 2023–2024, which reached a very high intensity level (Table 5, Figure 6).

For the 2023–2024 influenza season, the epidemic period, as estimated by MEM, started in week 42 of 2023 and lasted for 29 weeks. The pre- and post-epidemic thresholds were 0.08 and 0.18, respectively (Figure 7). The timeliness of epidemic detection was zero weeks. There was no detection lag for the 2023–2024 season. The peak intensity was estimated at a very high level in this season.

3.6 Stratification analysis by influenza strain

In the analysis of influenza virus types from the 2011–2012 to the 2023–2024 seasons, a total of 3,870 positive samples were recorded. A(H1N1)pdm09 and A(H3N2) are the **two** dominant influenza strains in Kunming, accounting for 74.54% of positive samples. A(H1N1)pdm09 has the highest peak PR of 47.76% and was prevalent across 5 seasons, making it the most consistently dominant strain. In contrast, B/Yamagata-lineage and B/Victoria-lineage played a smaller role, with B/Yamagata-lineage being more prevalent, reaching a maximum peak of 38.04%. The MEM estimates indicate that influenza outbreaks typically start in late autumn or early winter (weeks 44–48) and last for about 16–18 weeks. The epidemic thresholds vary, with A(H3N2) having the highest threshold of 3% and B/Yamagata-lineage the lowest at 1.49% (Table 6).

4 Discussion

This study is the first to validate the Moving Epidemic Method (MEM) for influenza surveillance in a subtropical plateau setting. The MEM model exhibited robust performance, with high sensitivity (74%) and specificity (87%) for detecting epidemics,

and no temporal lag in identifying the onset of the 2023–2024 influenza season. The epidemic threshold for the 2023–2024 season was determined at 8%, while subtype-specific thresholds varied markedly, 1.49–3%, underscoring distinct transmission dynamics among circulating strains. Notably, Kunming's threshold was substantially lower than those reported in other subtropical and tropical regions, such as Guangdong 11.99% and Wuhan 15.42% (24, 25), and even contrasted with the World Health Organization (WHO)-recommended baseline of 13.2% for tropical Cambodia (27). Although the exact impact is not yet clear (28–30), humidity, precipitation, and temperature are the primary climatic factors influencing tropical and subtropical regions. The spread of influenza in tropical and subtropical regions. Affected by the Kunming quasi-stationary front (31, 32), the climate in Kunming is sunny and dry during the winter and spring seasons. These discrepancies validate the adaptability of MEM in subtropical plateau environments but also emphasize the necessity of region-specific threshold calibration.

Spatiotemporal analysis revealed marked heterogeneity in influenza transmission across Kunming, with peripheral districts consistently exhibiting higher incidence rates than urban centers. Since 2018, overall influenza morbidity has sharply increased, culminating in a historical peak in 2023. This pattern suggests a potential exacerbation of pre-existing spatial inequalities in influenza burden, possibly reflecting disparities in healthcare access, population density, socioeconomic factors, or environmental conditions between urban core and peri-urban and rural regions. In parallel, cross-correlation analysis demonstrated that virological positivity rates (PR) consistently led reported incidence by ∼1 week, particularly in the post-COVID-19 period. These findings highlight PR as a reliable and timely indicator of early warning indicator for influenza activity.

PR data can better reflect the real-world influenza epidemic situation compared to syndromic indicators, such as ILI (33, 34). Since the identification of influenza-like illness also includes other

TABLE 3 Model fitting effect under different parameter settings.

Parameter δ	Sensitivity	Specificity	PPV	NPV	Youden index
1.0	0.52	0.90	0.75	0.77	0.43
1.1	0.74	0.87	0.76	0.86	0.61
1.2	0.70	0.89	0.78	0.84	0.59
1.3	0.67	0.90	0.79	0.83	0.57
1.4	0.68	0.90	0.79	0.83	0.58
1.5	0.68	0.90	0.79	0.83	0.58
1.6	0.68	0.90	0.79	0.83	0.58
1.7	0.67	0.91	0.80	0.83	0.58
1.8	0.64	0.91	0.81	0.82	0.55
1.9	0.63	0.93	0.83	0.82	0.56
2.0	0.52	0.94	0.83	0.78	0.46
2.1	0.48	0.94	0.83	0.76	0.43
2.2	0.48	0.94	0.83	0.76	0.42
2.3	0.42	0.96	0.85	0.75	0.38
2.4	0.42	0.96	0.85	0.74	0.38
2.5	0.37	0.97	0.88	0.73	0.34
2.6	0.34	0.98	0.89	0.72	0.32
2.7	0.34	0.98	0.89	0.72	0.32
2.8	0.31	0.97	0.85	0.71	0.28
2.9	0.31	0.97	0.85	0.71	0.28
3	0.29	0.97	0.85	0.71	0.26

YI, Youden's Index; PPV, Positive Predictive Value; NPV, Negative Predictive Value.

TABLE 4 Cross-validation results of influenza in Kunming before and after eliminating abnormal data from 2011–2012 to 2023–2024.

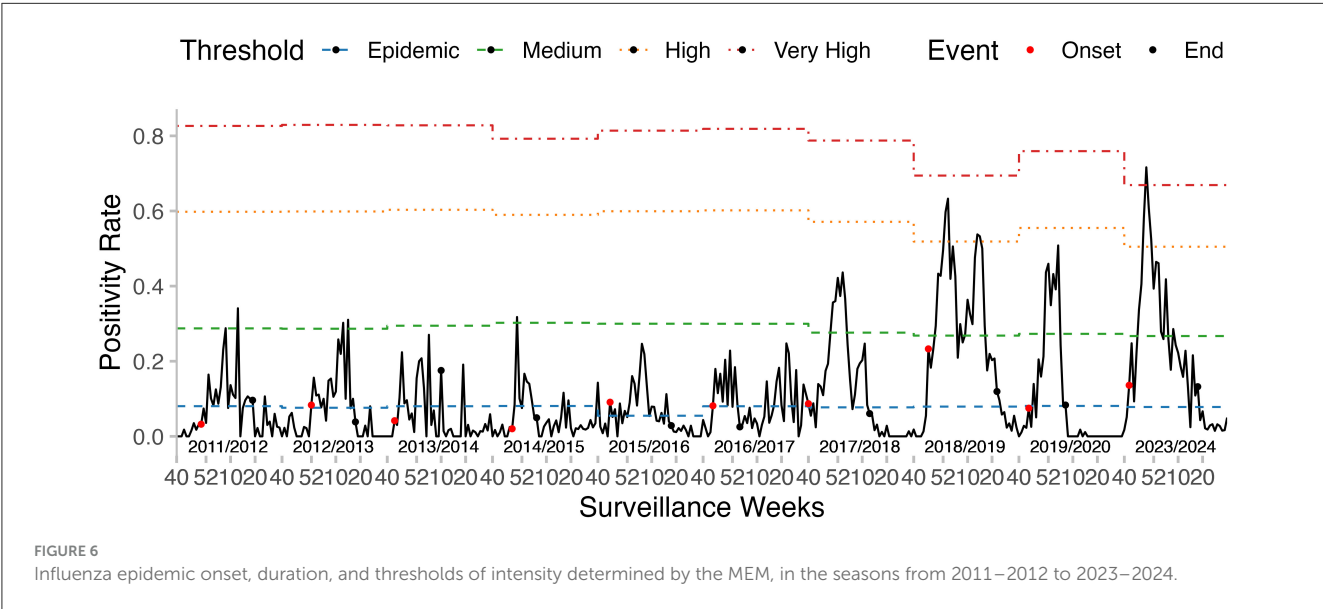| Season	Incorporate all data			Excluding the 2014–2015 season		
	Sensitivity	Specificity	YI	Sensitivity	Specificity	YI
2011–2012	0.73	0.90	0.63	0.73	0.90	0.63
2012–2013	0.87	0.87	0.74	0.87	0.87	0.74
2013–2014	0.64	0.86	0.50	0.64	0.86	0.50
2014–2015	0.20	0.99	0.19	–	–	–
2015–2016	0.59	0.85	0.44	0.59	0.85	0.44
2016–2017	0.86	0.63	0.49	0.94	0.58	0.52
2017–2018	0.86	0.78	0.63	0.88	0.76	0.64
2018–2019	0.98	0.53	0.51	0.99	0.51	0.50
2019–2020	0.89	0.97	0.86	0.89	0.97	0.86
2023–2024	0.93	0.67	0.60	0.96	0.65	0.61

YI, Youden's Index.

symptoms of viral infections, such as those caused by respiratory syncytial virus (RSV) and adenovirus (35–38). Therefore, virology-based data enhance specificity by minimizing confounding factors from non-influenza respiratory pathogens. Affected by the novel coronavirus, the PR has decreased in our surveillance data from 2020–2021 to 2022–2023. Our study, therefore, excluded these seasons at the beginning of data inclusion. Moreover, after the cross-validation process, the 2014–2015 season was removed due to its low sensitivity of 0.2. This low sensitivity might be attributed to poor surveillance quality, which led to false zero data occurring during the epidemic period. After the 2014–2015 season, we observed that the weekly PR values exhibited a more stable trend,

TABLE 5 Influenza epidemic onset, duration, thresholds of PR, and peak intensity level determined by the MEM from 2011−2012 to 2023−2024 seasons.

Seasons	Onset	Duration	Epidemic threshold (%)				
			Pre	Medium	High	Very high	Intensity
2011–2012	50	22	8.03	28.74	59.79	82.65	Medium
2012–2013	52	19	7.61	28.65	59.87	82.92	Medium
2013–2014	43	20	8.02	29.45	60.32	82.80	Low
2014–2015	48	11	8.08	30.23	58.97	79.23	Medium
2015–2016	45	26	5.49	29.98	59.93	81.39	Low
2016–2017	44	12	8.01	29.97	60.16	81.87	Low
2017–2018	40	26	7.72	27.61	57.11	78.75	Medium
2018–2019	46	29	7.92	26.82	51.87	69.42	High
2019–2020	44	16	8.10	27.29	55.48	75.93	Medium
2023–2024	42	29	7.81	26.70	50.48	66.89	Very high

FIGURE 6
Influenza epidemic onset, duration, and thresholds of intensity determined by the MEM, in the seasons from 2011−2012 to 2023−2024.

and the occurrence of zero values between epidemic periods became less frequent. Additionally, the peak PR values showed an upward trend, increasing from 24.63 to 71.62% after the 2015–2016 season. In the 2023–2024 season, the influenza epidemic entered a low-intensity phase at the 42nd week. Subsequently, it rapidly transitioned to a high-intensity phase at the 48th week and reached its peak at the 49th week, with a PR of 71.62%. The high-intensity influenza epidemic was also detected in Beijing (39), and the number of infections has tripled in the 2023–2024 season.

The Moving Epidemic Method (MEM) shows superior performance in modeling single-peak epidemics compared to dual-peak patterns (20). In Kunming, influenza virology data predominantly exhibited a unimodal distribution across the majority of the seasons. When the absolute humidity (AH) is relatively low, the survival and transmission of influenza viruses will increase (40), which corresponds to the peak of influenza activity observed every winter. However, during the 2017–2018

and 2018–2019 seasons, a bimodal pattern emerged, characterized by a primary winter peak followed by a secondary spring peak. During these two seasons, the H1N1(pdm09) was the predominant circulating strain, accounting for over 40%, which was consistent with similar research conducted in Wuhan and Guangdong (24, 25). The situation has an obvious discrepancy between the two seasons. In the 2017–2018 season, the overall positivity rate (PR) trend was consistent with that of H1N1(pdm09). In contrast, during the 2018–2019 season, the bimodal pattern was caused by the trend of H1N1(pdm09) followed by that of B/Yamagata. The antigenic shifts in circulating influenza strains, which alter herd immunity dynamics and may prolong transmission windows (41). Therefore, stratified research on influenza is also of great significance. Through stratification analysis, the predominant strain was the A-type epidemic strain, and the B/Yamagata epidemic strain was also superimposed in some years. The H1N1(pdm09) has persisted for more than five seasons. In these seasons, it accounted for over 45%, and the epidemic duration
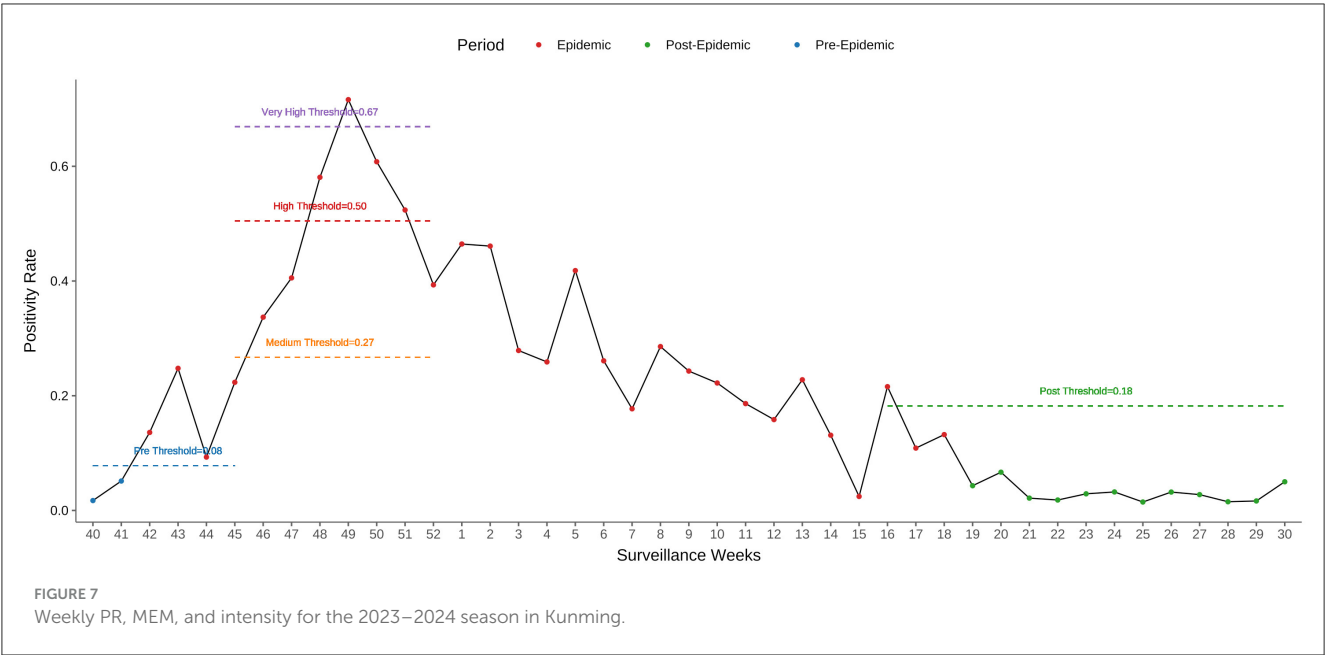
FIGURE 7
Weekly PR, MEM, and intensity for the 2023–2024 season in Kunming.

TABLE 6 Epidemics by influenza virus strain in Kunming from 2011–2012 to 2023–2024 seasons.

Influenza strain	Positive samples (n)	Percentage (%)	Maximum peak (%)	Moving epidemic model estimation			
				n of seasons	Start week	Epidemic length (weeks)	Epidemic threshold (%)
A(H1N1)pdm09	1,451	37.49	47.76	5	48	18	85
A(H3N2)	1,434	37.05	44.91	4	44	17	3
B/Yamagata-lineage	850	21.96	38.04	3	48	16	49
B/Victoria-lineage	135	59	27.27	1	44	–	–

in each of these seasons exceeded 20 weeks, determined by MEM. In contrast, when H3N2 became the predominant strain, the epidemic duration was 11–16 weeks, which was shorter than that of H1N1(pdm09). The B/Yamagata lineage mainly overlapped with the H3N2 strain during the 2023–2024 epidemic season. As for the B/Victoria lineage, it was only prevalent in the 2011–2012 season and not considered in MEM. The higher threshold for A(H3N2) (3%) compared to A(H1N1)pdm09 (2.85%) and B/Yamagata (1.49%) also reflects distinct transmission dynamics.

This study has several limitations. First, the generalizability of four sentinel sites might limit the findings to the urban city. The four sentinel surveillance sites were all located within Kunming's major district and remained unchanged from their establishment after the SARS outbreak in 2003 until 2024. This geographic concentration may limit the representativeness of our findings for the entire city, as the catchment areas of these sites do not fully encompass Kunming's diverse urban, peri-urban, and rural populations. Second, the limited representation of influenza B lineages precluded robust subtype-specific analyses. Third, the study did not include meteorological or population mobility data. Future research should integrate these factors to refine predictive models. Nevertheless, the absence of complementary data sources prevented us from exploring behavioral factors.

5 Conclusion

This study validates the MEM as a robust tool for influenza surveillance in subtropical plateau regions. By establishing localized thresholds and characterizing strain-specific dynamics, the findings support data-driven public health strategies aimed at mitigating the impact of seasonal influenza. Based on the MEM's performance, we recommend its integration into Kunming's routine influenza surveillance system. Subtype-specific thresholds should guide stratified responses, with increased vigilance during A(H3N2)-dominant seasons. Vaccination programs could be optimized by aligning administration with the typical onset of epidemics and prioritizing high-risk groups. Furthermore, the variability in B/Yamagata-lineage activity, coupled with its global decline after 2020, warrants continuous monitoring to assess potential resurgent risks. Future studies should focus on expanding data sources and exploring the applicability of MEM to other respiratory pathogens,

thereby reinforcing global health preparedness in the face of evolving viral threats.

Data availability statement

The data analyzed in this study is subject to the following licenses/restrictions: the dataset is part of Kunming CDC Notifiable Communicable Disease Reporting System and the National Immunization Program System. It is not publicly available according to the legislations. Requests to access the datasets should be directed to YG, gao_yudong@163.com.

Ethics statement

The studies involving humans were approved by Board of the Kunming Center for Disease Control and Prevention. The studies were conducted in accordance with the local legislation and institutional requirements. The human samples used in this study were acquired from a by-product of routine care or industry. Written informed consent for participation was not required from the participants or the participants' legal guardians/next of kin in accordance with the national legislation and institutional requirements.

Author contributions

YG: Writing – review & editing, Writing – original draft. YZ: Writing – review & editing, Visualization. SL: Data curation, Writing – review & editing. ZC: Writing – review & editing. YW: Writing – review & editing. ZZ: Writing – review & editing. XS: Funding acquisition, Writing – review & editing, Conceptualization, Supervision.

Funding

Conflict of interest

The authors declare that the research was conducted in the absence of any commercial or financial relationships that could be construed as a potential conflict of interest.

Generative AI statement

The author(s) declare that no Gen AI was used in the creation of this manuscript.

Publisher's note

References

1. Centers for Disease Control and Prevention (2025). *Types of Influenza Viruses*. Available from: https://www.cdc.gov/flu/about/viruses-types.html?CDC_AAref_Val; https://www.cdc.gov/flu/about/viruses/types.htm (accessed March 14, 2025).

2. Boattini M, Charrier L, Almeida A, Christaki E, Moreira Marques T, Tosatto V, et al. Burden of primary influenza and respiratory syncytial virus pneumonia in hospitalised adults: insights from a 2-year multi-centre cohort study (2017-2018). *Intern Med J*. (2023) 53:404–8. doi: 10.1111/imj.15583

3. Iuliano AD, Roguski KM, Chang HH, Muscatello DJ, Palekar R, Tempia S, et al. Estimates of global seasonal influenza-associated respiratory mortality: a modelling study. *Lancet*. (2018) 391:1285–300. doi: 10.1016/S0140-6736(17)33293-2

4. Langer J, Welch VL, Moran MM, Cane A, Lopez SMC, Srivastava A, et al. High Clinical Burden of Influenza Disease in Adults Aged >/= 65 Years: Can We Do Better? A systematic literature review. *Adv Ther*. (2023) 40:1601–27. doi: 10.1007/s12325-023-02432-1

5. Wang X, Li Y, O'Brien KL, Madhi SA, Widdowson MA, Byass P, et al. Global burden of respiratory infections associated with seasonal influenza in children under 5 years in 2018: a systematic review and modelling study. *Lancet Glob Health*. (2020) 8:e497–510. doi: 10.1016/S2214-109X(19)30545-5

6. Macias AE, McElhaney JE, Chaves SS, Nealon J, Nunes MC, Samson SI, et al. The disease burden of influenza beyond respiratory illness. *Vaccine*. (2021) 39:A6–A14. doi: 10.1016/j.vaccine.2020.09.048

7. National Administration of Disease Control and Prevention (2023). *General Situation of Legal Infectious Diseases in China in 2023*. Available from: https://www.

ndcpa.gov.cn/jbkzzx/c100016/common/content/content_1836299733133275136.html (accessed March 14, 2025).

8. Li J, Chen Y, Wang X, Yu H. Influenza-associated disease burden in mainland China: a systematic review and meta-analysis. *Sci Rep*. (2021) 11:2886. doi: 10.1038/s41598-021-82161-z

9. World Health Organization (2025). *Influenza (seasonal)*. Available from: https://www.who.int/news-room/fact-sheets/detail/influenza-(seasonal) (accessed March 14, 2025).

10. Chen Z, Tsui JL, Gutierrez B, Busch Moreno S, du Plessis L, Deng X, et al. COVID-19 pandemic interventions reshaped the global dispersal of seasonal influenza viruses. *Science*. (2024) 386:eadq3003. doi: 10.1126/science.adq3003

11. Ryu S, Cowling BJ. Human Influenza Epidemiology. *Cold Spring Harb Perspect Med*. (2021) 11:a038356. doi: 10.1101/cshperspect.a038356

12. Wille M, Holmes EC. The ecology and evolution of influenza viruses. *Cold Spring Harb Perspect Med*. (2020) 10:a038489. doi: 10.1101/cshperspect.a038489

13. Neumann G, Kawaoka Y. Seasonality of influenza and other respiratory viruses. *EMBO Mol Med*. (2022) 14:e15352. doi: 10.15252/emmm.202115352

14. Hirve S, Newman LP, Paget J, Azziz-Baumgartner E, Fitzner J, Bhat N, et al. Influenza seasonality in the tropics and subtropics—when to vaccinate? *PLoS ONE*. (2016) 11:e0153003. doi: 10.1371/journal.pone.0153003

15. Cheng X, Tan Y, He M, Lam TT, Lu X, Viboud C, et al. Epidemiological dynamics and phylogeography of influenza virus in southern China. *J Infect Dis*. (2013) 207:106–14. doi: 10.1093/infdis/jis526

16. Petrova VN, Russell CA. The evolution of seasonal influenza viruses. *Nat Rev Microbiol.* (2018) 16:47–60. doi: 10.1038/nrmicro.2017.118

17. Tamerius J, Nelson MI, Zhou SZ, Viboud C, Miller MA, Alonso WJ. Global influenza seasonality: reconciling patterns across temperate and tropical regions. *Environ Health Perspect.* (2011) 119:439–45. doi: 10.1289/ehp.1002383

18. Zhang H, Wang L, Lai S, Li Z, Sun Q, Zhang P. Surveillance and early warning systems of infectious disease in China: From 2012 to 2014. *Int J Health Plann Manage.* (2017) 32:329–38. doi: 10.1002/hpm.2434

19. Cengiz Ü, Karahasan M, A. new statistical early outbreak detection method for biosurveillance and performance comparisons. *Stat Med.* (2019) 38:5236–58. doi: 10.1002/sim.8368

20. Vega T, Lozano JE, Meerhoff T, Snacken R, Mott J, Ortiz de. Lejarazu R, et al. Influenza surveillance in Europe: establishing epidemic thresholds by the moving epidemic method. *Influenza Other Respir Viruses.* (2013) 7:546–58. doi: 10.1111/j.1750-2659.2012.00422.x

21. Murray JLK, Marques DFP, Cameron RL, Potts A, Bishop J, von Wissmann B, et al. Moving epidemic method (MEM) applied to virology data as a novel real time tool to predict peak in seasonal influenza healthcare utilisation. The Scottish experience of the 2017/18 season to date. *Euro Surveill.* (2018) 23:18-00079. doi: 10.2807/1560-7917.ES.2018.23.11.18-00079

22. Rakocevic B, Grgurevic A, Trajkovic G, Mugosa B, Sipetic Grujicic S, Medenica S, et al. Influenza surveillance: determining the epidemic threshold for influenza by using the Moving Epidemic Method (MEM), Montenegro, 2010/11 to 2017/18 influenza seasons. *Euro Surveill.* (2019) 24:1800042. doi: 10.2807/1560-7917.ES.2019.24.12.1800042

23. Vega T, Lozano JE, Meerhoff T, Snacken R, Beaute J, Jorgensen P, et al. Influenza surveillance in Europe: comparing intensity levels calculated using the moving epidemic method. *Influenza Other Respir Viruses.* (2015) 9:234–46. doi: 10.1111/irv.12330

24. Jiang Y, Tong YQ, Fang B, Zhang WK, Yu XJ. Applying the moving epidemic method to establish the influenza epidemic thresholds and intensity levels for age-specific groups in Hubei Province, China. *Int J Environ Res Public Health.* (2022) 19:1677. doi: 10.3390/ijerph19031677

25. Kang M, Tan X, Ye M, Liao Y, Song T, Tang S. The moving epidemic method applied to influenza surveillance in Guangdong, China. *Int J Infect Dis.* (2021) 104:594–600. doi: 10.1016/j.ijid.2021.01.058

26. Wang D, Guerra A, Wittke F, Lang JC, Bakker K, Lee AW, et al. Real-time monitoring of infectious disease outbreaks with a combination of google trends search results and the moving epidemic method: a respiratory syncytial virus case study. *Trop Med Infect Dis.* (2023) 8:75. doi: 10.3390/tropicalmed8020075

27. Ly S, Arashiro T, Ieng V, Tsuyuoka R, Parry A, Horwood P, et al. Establishing seasonal and alert influenza thresholds in Cambodia using the WHO method: implications for effective utilization of influenza surveillance in the tropics and subtropics. *Western Pac Surveill Response J.* (2017) 8:22–32. doi: 10.5365/wpsar.2017.8.1.002

28. Tamerius JD, Shaman J, Alonso WJ, Bloom-Feshbach K, Uejio CK, Comrie A, et al. Environmental predictors of seasonal influenza epidemics across temperate and tropical climates. *PLoS Pathog.* (2013) 9:e1003194. doi: 10.1371/journal.ppat.1003194

29. Shek LP, Lee BW. Epidemiology and seasonality of respiratory tract virus infections in the tropics. *Paediatr Respir Rev.* (2003) 4:105–11. doi: 10.1016/S1526-0542(03)00024-1

30. Lowen AC, Steel J. Roles of humidity and temperature in shaping influenza seasonality. *J Virol.* (2014) 88:7692–5. doi: 10.1128/JVI.03544-13

31. Du X, Dai H, Cao J, Tao Y, Yu J. Interannual variability of the occurrence frequency of the stronger Kunming quasi-stationary front in winter. *Int J Climatol.* (2024) 44:4178–91. doi: 10.1002/joc.8575

32. Zhao D, Yang R, Tao Y, Zhang WK, He X. Objective detection of the Kunming quasi-stationary front. *Theor Appl Climatol.* (2019) 138:1405–18. doi: 10.1007/s00704-019-02894-w

33. Raad C, Ouldali N, Lebel M, Paquette M, Gilca R, Papenburg J, et al. Use of the moving epidemic method to guide the launch of palivizumab immunization campaigns for respiratory syncytial virus in Quebec, Canada. *Can J Public Health.* (2024). doi: 10.17269/s41997-024-00985-4

34. Khaleel HA, Alhilfi RA, Rawaf S, Tabche C. Identify future epidemic threshold and intensity for influenza-like illness in Iraq by using the moving epidemic method. *IJID Reg.* (2024) 10:126–31. doi: 10.1016/j.ijregi.2023.12.005

35. Gertz A, Rader B, Sewalk K, Varrelman TJ, Smolinski M, Brownstein JS. Decreased seasonal influenza rates detected in a crowdsourced influenza-like illness surveillance system during the COVID-19 pandemic: prospective cohort study. *JMIR Public Health Surveill.* (2023) 9:e40216. doi: 10.2196/40216

36. Wang C, Yang YN Xi L, Yang LL, Du J, Zhang ZS, et al. Dynamics of influenza-like illness under urbanization procedure and COVID-19 pandemic in the subcenter of Beijing during 2013-2021. *J Med Virol.* (2022) 94:3801–10. doi: 10.1002/jmv.27803

37. Ceccarelli G. d'Ettorre G, Russo A, Fabris S, Ciccozzi M, d'Ettorre G. SARS-CoV-2 pandemic, influenza, and influenza-like illness epidemics: Allies or enemies? *J Med Virol.* (2023) 95:e28148. doi: 10.1002/jmv.28148

38. Kovacevic A, Eggo RM, Baguelin M, Domenech de Celles M, Opatowski L. The impact of cocirculating pathogens on severe acute respiratory syndrome coronavirus 2 (SARS-CoV-2)/Coronavirus Disease 2019 Surveillance: How Concurrent Epidemics May Introduce Bias and Decrease the Observed SARS-CoV-2 Percentage Positivity. *J Infect Dis.* (2022) 225:199–207. doi: 10.1093/infdis/jiab459

39. Zhu W, Gu L. Resurgence of seasonal influenza driven by A/H3N2 and B/Victoria in succession during the 2023-2024 season in Beijing showing increased population susceptibility. *J Med Virol.* (2024) 96:e29751. doi: 10.1002/jmv.29751

40. Shaman J, Kohn M. Absolute humidity modulates influenza survival, transmission, and seasonality. *Proc Natl Acad Sci U S A.* (2009) 106:3243–8. doi: 10.1073/pnas.0806852106

41. Sandbulte MR, Westgeest KB, Gao J, Xu X, Klimov AI, Russell CA, et al. Discordant antigenic drift of neuraminidase and hemagglutinin in H1N1 and H3N2 influenza viruses. *Proc Natl Acad Sci U S A.* (2011) 108:20748–53. doi: 10.1073/pnas.1113801108